

# Ionic Hydrogen Bonds in Bioenergetics. 3. Proton Transport in Membranes, Modeled by Ketone/Water Clusters

Michael Meot-Ner (Mautner),\*<sup>†</sup> Steve Scheiner,<sup>‡</sup> and Wa On Yu<sup>‡</sup>

Contribution from the Physical and Chemical Properties Division, National Institute of Standards and Technology, Gaithersburg, Maryland 20899, Department of Chemistry, University of Canterbury, Christchurch 8001, New Zealand, and Department of Chemistry and Biochemistry, Southern Illinois University, Carbondale, Illinois 62901-4409

Received May 21, 1997

**Abstract:** Hydrogen bond networks in protonated acetone/water clusters are stabilized by  $\text{H}_3\text{O}^+(\text{Me}_2\text{CO})_2$  centers, and the stabilization increases with further acetone content. For example, proton transfer from neat water  $(\text{H}_2\text{O})_6\text{H}^+$  clusters to form mixed  $(\text{Me}_2\text{CO})_3(\text{H}_2\text{O})_3\text{H}^+$  clusters is exothermic by 80 kJ/mol (19 kcal/mol), due to strong hydrogen bonding of the carbonyl groups; in a series of mixed clusters  $\text{B}_3(\text{H}_2\text{O})_3\text{H}^+$ , the stability of the hydrogen bond network correlates with the proton affinities PA(B). In diketone models of adjacent peptide links, the proton is stabilized by internal hydrogen bonds between the carbonyl groups. The internal bonds can be significant, for example, 31 kJ/mol (7 kcal/mol) in  $(\text{MeCOCH}_2\text{CH}_2\text{COMe})\text{H}^+$ , but proton transfer through the internal bond has a high barrier. However, water molecules can bridge between the CO groups. In these bridges, the proton remains on an  $\text{H}_3\text{O}^+$  center, in both acetone/water and diketone/water systems. With a further  $\text{H}_2\text{O}$  molecule, the diketone/water cluster  $(\text{MeCOCH}_2\text{CH}_2\text{COMe})(\text{H}_2\text{O})_2\text{H}^+$  and diamide/water clusters form two-water  $\text{H}_3\text{O}^+\cdots\text{H}_2\text{O}$  bridges, which allow proton transfer between the CO groups with a small barrier of <12 kJ/mol (<3 kcal/mol). The cluster models suggest several roles for hydrogen bonds in proton transport through membranes. (1) Ionic hydrogen bonds involving polar amide groups stabilize ions by up to 135 kJ/mol (32 kcal/mol) in clusters and can similarly stabilize ions in membrane water chains and enzyme centers. (2) The proton can remain on an  $\text{H}_3\text{O}^+$  center and, therefore, remain delocalized and mobile in water chains, despite the stronger basicities of the surrounding amide groups. This effect results from electrostatic balancing of opposing peptide amide dipoles. (3) In the water chains,  $\text{H}_3\text{O}^+\cdots\text{H}_2\text{O}$  bridges between peptide amide groups can provide low-energy pathways for proton transport.

## Introduction

Cluster studies can help quantify the energetics and structure of protonated hydrogen bond assemblies. For example, cluster studies showed that in  $\text{B}_n(\text{H}_2\text{O})_m\text{H}^+$  clusters the proton remains on an  $\text{H}_3\text{O}^+$  core ion, even if B is a strong intrinsic base, when this structure allows a network of strong  $\text{OH}^+\cdots\text{O}$  hydrogen bonds.<sup>1–3</sup> An  $\text{H}_3\text{O}^+$  core ion applies also in more complex environments of polyfunctional molecules such as crown ethers and polyethers,<sup>4,5</sup> and it may participate in protonated bridges containing two water molecules in polyether/water clusters.<sup>5</sup>

Similar to clusters, ions in protein interiors are in partially hydrated environments and they interact strongly with intracavity water molecules and with polar groups. For example, we measured the bonding of anions to imidazole and peptide amide NH groups in cluster models of enzyme reactions. The preceding papers in this series showed that ionic hydrogen bonds can stabilize anionic intermediates by as much as 134 kJ/mol (32 kcal/mol) because the peptide NH groups are strong intrinsic acids and, therefore, serve as strong hydrogen donors in  $\text{NH}\cdots\text{O}^-$  bonds.<sup>6,7</sup>

Similarly, peptide amide CO groups are strong intrinsic bases and can be efficient hydrogen acceptors in cationic  $\text{OH}^+\cdots\text{OC}$  hydrogen bonds. The significance of ionic interactions with the polar environment was pointed out by Warshel<sup>8–11</sup> in relation to proton transport through water wires.<sup>8–17</sup> Clusters can indicate the contributions of specific energy components, in particular, the contributions of ionic hydrogen bonds, and can help to calibrate computations of more complex biosystems. Of course, in complex systems, the various energy factors interact and cannot be measured separately experimentally. However, some of the effects of the complex system on the hydrogen bond components can be estimated from known trends in cluster energetics, as described in the Appendix. With these corrections, the cluster data can provide mechanistic insights into the roles of hydrogen bonds and give a measure of its contributions.

(6) Meot-Ner (Mautner), M. *J. Am. Chem. Soc.* **1988**, *110*, 3071 (first paper in the present series).

(7) Meot-Ner (Mautner), M. *J. Am. Chem. Soc.* **1988**, *110*, 3075 (second paper in the present series).

(8) Warshel, A. *Proc. Natl. Acad. Sci.* **1978**, *75*, 2558.

(9) Warshel, A. *Photochem. Photobiol.* **1979**, *30*, 290.

(10) Warshel, A. *Methods Enzymol.* **1988**, *127*, 578.

(11) Aqvist, J.; Warshel, A. *Biophys. J.* **1989**, *56*, 171.

(12) Deamer, D. W. *J. Bioenerg. Biomembr.* **1987**, *19*, 457.

(13) Onsager, L. In *Physical Principles of Biological Membranes*; Snell, F., Wolken, J., Iverson, G., Lam, J., Eds.; Gordon and Breach: New York, 1970; p 137.

(14) Nagle, J. F.; Tristram-Nagle, S. *J. Membr. Biol.* **1983**, *74*, 1.

(15) Deamer, D. W.; Nichols, J. W. *J. Membr. Biol.* **1989**, *107*, 91.

(16) Finney, J. L. *Phil. Trans. R. Soc. London B* **1977**, *278*, 3.

(17) Kasianowitz, J.; McLaughlin, S. *J. Membr. Biol.* **1987**, *95*, 73.

\* Address correspondence to this author at University of Canterbury.

<sup>†</sup> National Institute of Standards and Technology and University of Canterbury.

<sup>‡</sup> Southern Illinois University.

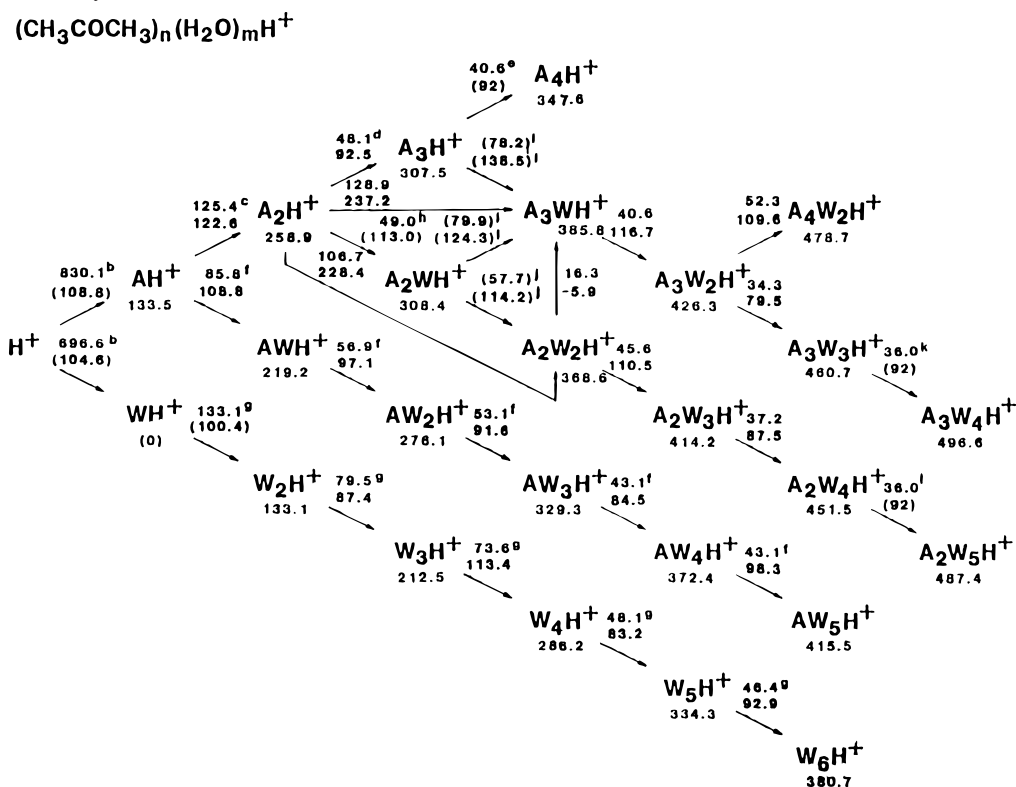
(1) Keesee, R. G.; Castleman, A. W. *J. Phys. Chem. Ref. Data* **1986**, *15*, 1011.

(2) Kebarle, P. *Annu. Rev. Phys. Chem.* **1977**, *28*, 445.

(3) Meot-Ner (Mautner), M. *J. Am. Chem. Soc.* **1984**, *106*, 1257, 1265.

(4) Sharma, R. B.; Kebarle, P. *J. Am. Chem. Soc.* **1984**, *106*, 3913.

(5) Meot-Ner (Mautner), M.; Sieck, L. W.; Duan, X. F.; Scheiner, S. *J. Am. Chem. Soc.* **1994**, *116*, 7848.

Table 1. Thermochemistry<sup>a</sup> of Acetone/Water Mixed Clusters A<sub>n</sub>W<sub>m</sub>H<sup>+</sup>

<sup>a</sup> Top number above arrow is  $-\Delta H^\circ$  in kJ/mol; bottom number is  $-\Delta S^\circ$  in J/(mol K). Number under formula is stability in terms of dissociation to the highest energy monomers  $WH^+ + mA + (n-1)W$ .  $\Delta S^\circ$  values in parentheses are estimated. For individual temperature studies, uncertainty estimates  $u_i$  for the thermochemical values are derived from the standard deviations of the slopes and intercepts of the van't Hoff plots (of  $n$  points) multiplied by the 95% confidence interval coefficients from Student's  $t$ -distribution for  $n-2$  degrees of freedom. For the two-step equilibria measured over a short temperature range, the calculated uncertainty is multiplied by an additional coverage factor of 2 to obtain the values quoted in the table. For results obtained from  $m$  determinations, the average value is assigned an uncertainty equal to  $(\sum u_i^2)^{1/2}/m$ . As another measure of the precision, the average standard deviation of the replicate  $\Delta H^\circ$  values was  $\pm 2.6$  kJ/mol ( $\pm 0.6$  kcal/mol) and of the  $\Delta S^\circ$  values was  $\pm 10.6$  J/(mol K) ( $\pm 2.5$  cal/mol K). Uncertainty estimates for  $\Delta H^\circ$  (kJ/mol) and  $\Delta S^\circ$  (J/(mol K)) and number of determinations:  $A_2H^+ + W$ , 2.1, 8.4, 6;  $A_2H^+ + A$ , 5.0, 19.2, 1;  $A_2H^+ + 2W$ , 6.7, 23.4, 3;  $A_2H^+ + A + W$ , 10.0, 33.5, 5;  $A_2W_2H^+ + W$ , 2.1, 7.5, 2;  $A_3WH^+ + W$ , 2.9, 13.4, 1;  $A_2W_3H^+ + W$ , 4.2, 17.2, 1;  $A_3W_2H^+ + W$ , 3.8, 16.7, 1;  $A_3W_2H^+ + A$ , 6.7, 28.9, 1. <sup>b</sup> Protonation thermochemistry from refs 18, 30, and 31. <sup>c</sup> Average of present work and literature values from ref 1. <sup>d</sup> Present work; compare with  $\Delta H^\circ = -51.0$  kJ/mol and  $\Delta S^\circ = -96.2$  J/(mol K) from refs 46 and 47. <sup>e</sup> From  $\Delta G^\circ_{215} = -20.9$  kJ/mol,  $\Delta S^\circ$  estimated as shown. Compare with  $\Delta H^\circ = -35.6$  kJ/mol and  $\Delta S^\circ = -71$  J/(mol K) from refs 46. <sup>f</sup> From ref 3. <sup>g</sup> From ref 34. <sup>h</sup> From  $\Delta G^\circ_{278} = -17.6$  kJ/mol. <sup>i</sup> From  $A_2H^+ \rightarrow A_3WH^+$  two-step addition and thermochemical cycle. <sup>j</sup> From  $A_2H^+ \rightarrow A_2W_2H^+$  two-step addition and thermochemical cycle. The result agrees well with  $\Delta H^\circ = -56.9$  kJ/mol, from  $\Delta G^\circ_{293} = -25.9$  kJ/mol and  $\Delta S^\circ$  estimated as shown. <sup>k</sup> From  $\Delta G^\circ_{224} = -15.1$  kJ/mol. <sup>l</sup> From  $\Delta G^\circ_{231} = -15.1$  kJ/mol.

This paper presents the thermochemistry and its structural implications in acetone/water clusters in section 1, diketone/water clusters in section 2, and ab initio calculations on model clusters in section 3. The implications for membrane transport are discussed in section 4 and in the Appendix.

### Experimental and Computational Methods

The measurements were performed using a NIST pulsed, high-pressure mass spectrometer. The experimental method and apparatus were described recently in detail.<sup>18</sup> Mixtures of H<sub>2</sub>O, ketone, and trace CHCl<sub>3</sub> as an electron capture agent in N<sub>2</sub> carrier gas were prepared in a 3-L bulb heated to 150 °C. The mixtures were allowed to flow to the ion source through stainless steel and glass lines also heated to 150 °C. The total pressure in the ion source was 2–4 mbar, containing 0.005–0.05 mbar of H<sub>2</sub>O and 0.0001–0.0005 mbar of ketone. The mixtures were ionized by 1-ms pulses of 1000-eV electrons. The ion signal corresponding to the various ions was observed at 2–10 ms, and constant product/reactant ion ratios assured that equilibrium was achieved.

The samples were from commercial sources and used as purchased. No impurity effects were noted. At the concentrations used, impurities of <2% would have no significant effects.

An anomaly was noted in the  $(Me_2CO)_2(H_2O)H^+$  cluster. In clustering sequences, equilibrium measurements are optimal when the concentration ratios of the consecutive clusters are  $<1$ , in which case a small degree of dissociation outside the ion source causes only small errors.<sup>19</sup> However, in this cluster, the thermochemistry of the consecutive steps leads to ion intensity ratios  $[(Me_2CO)_2(H_2O)_2H^+]/[(Me_2CO)_2(H_2O)H^+] > 1$  under all practical conditions. In this case, even a small amount of dissociation can lead to a significant error in the measured ion ratio.<sup>19</sup> Similar problems may have caused the unusual results reported by Hiraoka et al. for  $((Me_2O)(H_2O)_2)H^+$  which lead to inconsistent thermochemical cycles.<sup>20</sup> Therefore, for  $(Me_2CO)_2(H_2O)H^+$ , we used the  $\Delta G^\circ$  value obtained at the highest usable temperature where the effect is smallest, and  $\Delta H^\circ$  was calculated using an estimated  $\Delta S^\circ$  value. For the subsequent clusters, we bridged over this reaction and measured directly the two-step additions shown in Table 1 below. As a check on the accuracy of two-step equilibria, we also measured

(19) For an association reaction  $BH^+ + B \rightarrow BH^+ \cdot B$  with equilibrium ion ratio  $K_{ion} = [BH^+ \cdot B]/[BH^+]$ , if a fraction  $\alpha$  of  $BH^+ \cdot B$  dissociates to  $BH^+$  and  $B$  outside the source, the detected apparent equilibrium ratio  $K'_{ion}$  changes so that  $K'_{ion}/K_{ion} = (1 - \alpha)/(1 + \alpha K_{ion})$ . If the monomer  $BH^+$  is small, even a small contribution from  $BH^+ \cdot B$  can cause a relatively large error. Therefore, the error is negligible for small  $K_{ion}$  but becomes substantial for large  $K_{ion}$ . For example, if 0.01 of  $BH^+ \cdot B$  dissociates, the error in  $K_{ion}$  is 1% for  $K_{ion} = 0.01$ , 2% for  $K_{ion} = 1$ , but 50% for  $K_{ion} = 99$ .

(20) Hiraoka, K.; Grimsrud, E. P.; Kebarle, P. *J. Am. Chem. Soc.* **1974**, *96*, 3359.

(18) Meot-Ner (Mautner), M.; Sieck, L. W. *J. Am. Chem. Soc.* **1991**, *113*, 4448.

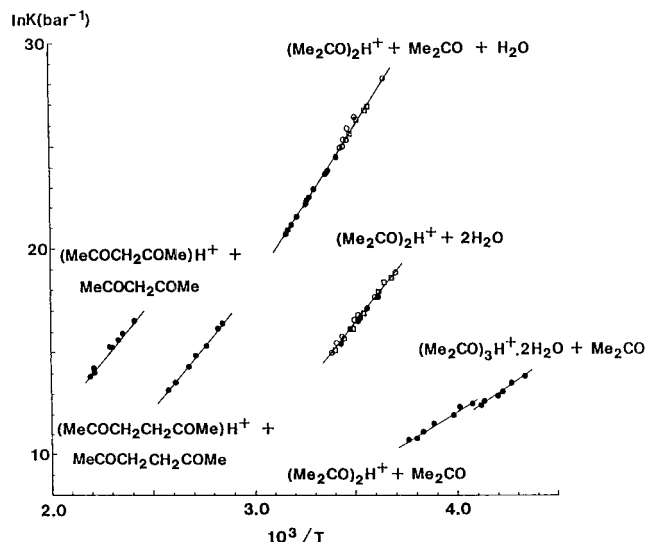


**Figure 1.** Van't Hoff plots for clustering reactions. Plots for the two-step equilibria show data from several replicate temperature studies.

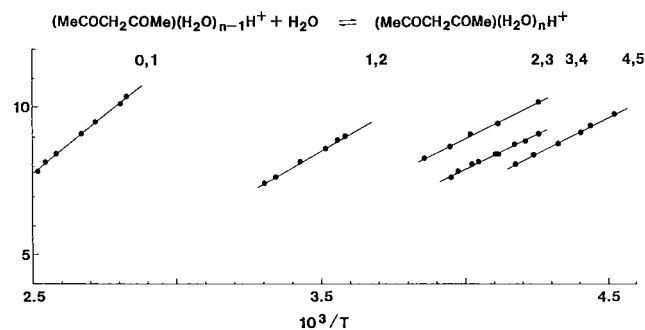


**Figure 2.** Van't Hoff plots for clustering reactions.

a two-step equilibrium in a system where the individual steps show no anomaly, i.e. for  $(\text{MeCOCH}_2\text{CH}_2\text{COMe})(\text{H}_2\text{O})\text{H}^+ + 2\text{H}_2\text{O}$ . These results agree well with the sum of the corresponding two individual steps, as shown in Table 1.

All calculations were carried out using the ab initio Gaussian-92 code.<sup>21</sup> The 4-31G basis set was used, and all geometries were fully optimized at the SCF level, using the standard Berny algorithms in Gaussian and the "verytight" convergence criteria.<sup>22</sup> The 4-31G basis set was chosen both for computational efficiency and for its ability to deal with hydrogen bonds and proton-transfer energetics satisfactorily.<sup>23,24</sup> Further features of the method will be discussed below.

## Results and Discussion

**1. Acetone/Water Clusters.** Van't Hoff plots for the clustering reactions are shown in Figures 1–4, and the results are summarized in Table 1 for the acetone/water system.

Uncertainty estimates for individual temperature studies are derived as described in footnote *a* of Table 1. Seven of the temperature studies were replicated 2–9 times, with reactant concentrations that varied up to a factor of 10, with reproducibility as described in footnote *a* of Table 1.

The energies of the hydrogen bond networks in the clusters can be expressed as the energy  $\Delta H_1^\circ$  required for decomposition

(21) Frisch, M. J.; Trucks, G. W.; Schlegel, H. B.; Gill, P. M. W.; Johnson, G. G.; Wong, M. W.; Foresman, J. B.; Robb, M. A.; Head-Gordon, M.; Replogle, E. S.; Bomperts, R.; Andres, J. L.; Ragavachari, K.; Binkley, J. S.; Gonzalez, G.; Martin, R. L.; Fox, D. J.; Defrees, D. J.; Baker, J.; Stewart, J. J. P.; Pople, J. A. Gaussian, Inc., Pittsburgh, PA, 1993.

(22) Ditchfield, R.; Hehre, W. J.; Pople, J. A. *J. Chem. Phys.* **1971**, *54*, 724; Schlegel, H. B. *J. Comput. Chem.* **1982**, *3*, 214.

(23) Cybulski, S. M.; Scheiner, S. *J. Phys. Chem.* **1990**, *94*, 6106.

(24) Scheiner, S. *Acc. Chem. Res.* **1985**, *18*, 174.

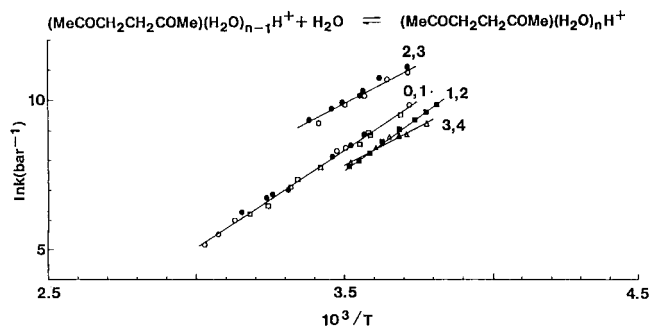
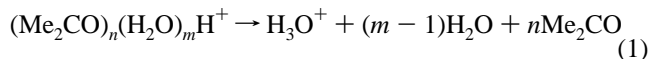


**Figure 3.** Van't Hoff plots for clustering reactions.

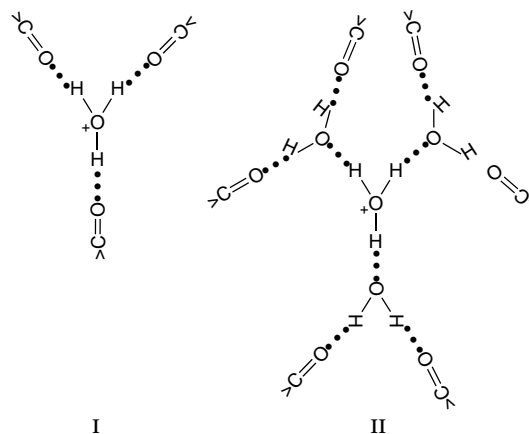
to the highest energy monomers.



These energies are pertinent because the core ion is  $\text{H}_3\text{O}^+$ , and we are interested in its stabilization by the hydrogen-bonded assembly. The cluster dissociation energies are shown under the formulas in Table 1. For clusters of a constant rank (i.e., constant  $n+m$ ), the stabilities of the hydrogen bond systems increase with increasing acetone content, in particular in introducing the first two acetone molecules. This may result from cooperative effects when two  $\text{Me}_2\text{CO}$  molecules bond to an  $\text{H}_3\text{O}^+$  center, similar to the  $(\text{MeCN})_2(\text{H}_2\text{O})\text{H}^+$  cluster.<sup>25</sup>

Interestingly, the  $(\text{Me}_2\text{CO})_2(\text{H}_2\text{O})\text{H}^+$  group seems to be particularly stable even in the presence of several further molecules. This is indicated by the energies of consecutive substitutions of  $\text{H}_2\text{O}$  by  $\text{Me}_2\text{CO}$  (progressing vertically up in Table 1), which have especially large effects for the first two steps. For example, even in the largest, six-membered clusters, consecutive substitutions in the series  $(\text{H}_2\text{O})_6\text{H}^+$ ,  $(\text{Me}_2\text{CO})(\text{H}_2\text{O})_5\text{H}^+$ , ...,  $(\text{Me}_2\text{CO})_4(\text{H}_2\text{O})_2\text{H}^+$  are exothermic by 34.8 and 36.0 kJ/mol (8.3 and 8.6 kcal/mol) for the first two substitutions, but only by 9.2 and 18.0 kJ/mol (2.2 and 4.3 kcal/mol) for the next two substitutions, respectively.

The stabilities increase in all the clusters of the same rank with additional acetone content, up to clusters with compositions  $(\text{Me}_2\text{CO})_{n+2}(\text{H}_2\text{O})_n\text{H}^+$ , where all the  $\text{H}_2\text{O}$  hydrogen-bonding sites are occupied, similar to  $\text{Me}_2\text{O}/\text{H}_2\text{O}$  and  $\text{MeCN}/\text{H}_2\text{O}$  clusters.<sup>20,25</sup> In analogy, the present thermochemistry suggests structures with protonated water in the center and blocked acetone molecules in the periphery, as in structures I and II.



(25) Deakyne, C. A.; Meot-Ner (Mautner), M.; Campbell, C. L.; Hughes, M. G.; Murphy, S. P. *J. Chem. Phys.* **1986**, *90*, 4648.

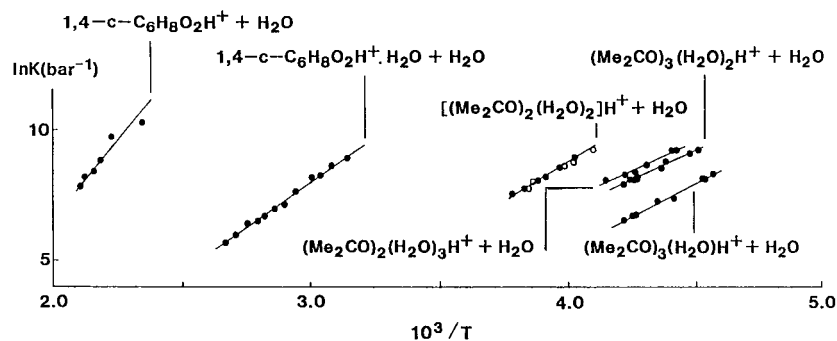


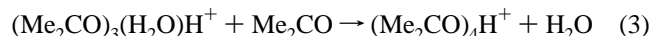
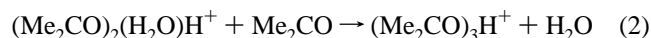
Figure 4. Van't Hoff plots for clustering reactions.

Table 2. Thermochemistry of Association Reactions<sup>a</sup>

	-ΔH°		-ΔS°	
	kJ/mol	kcal/mol	J/(mol K)	cal/(mol K)
1. (MeCOCH <sub>2</sub> COMe)H <sup>+</sup> + MeCOCH <sub>2</sub> COMe	108.8	26.0	123.0	29.4
2. (MeCOCH <sub>2</sub> COMe)H <sup>+</sup> + H <sub>2</sub> O	66.5	15.9	103.0	24.6
3. (MeCOCH <sub>2</sub> COMe)(H <sub>2</sub> O)H <sup>+</sup> + H <sub>2</sub> O	46.9	11.2	92.5	22.1
4. (MeCOCH <sub>2</sub> COMe)(H <sub>2</sub> O) <sub>2</sub> H <sup>+</sup> + H <sub>2</sub> O	39.7	9.5	84.9	20.3
5. (MeCOCH <sub>2</sub> COMe)(H <sub>2</sub> O) <sub>3</sub> H <sup>+</sup> + H <sub>2</sub> O	37.7	9.0	85.4	20.4
6. (MeCOCH <sub>2</sub> COMe)(H <sub>2</sub> O) <sub>4</sub> H <sup>+</sup> + H <sub>2</sub> O	40.6	9.7	102.1	24.4
7. (MeCOCH <sub>2</sub> COMe)(H <sub>2</sub> O) <sub>5</sub> H <sup>+</sup> + H <sub>2</sub> O	38.9 <sup>b</sup>	9.3 <sup>b</sup>	(105)	(25)
8. (MeCOCH <sub>2</sub> CH <sub>2</sub> COMe)H <sup>+</sup> + MeCOCH <sub>2</sub> CH <sub>2</sub> COMe	94.1	22.5	133.8	32.0
9. (MeCOCH <sub>2</sub> CH <sub>2</sub> COMe)H <sup>+</sup> + H <sub>2</sub> O	54.4	13.0	122.2	29.2
10. (MeCOCH <sub>2</sub> CH <sub>2</sub> COMe)(H <sub>2</sub> O)H <sup>+</sup> + H <sub>2</sub> O	54.8	13.1	125.5	30.0
11. (MeCOCH <sub>2</sub> CH <sub>2</sub> COMe)(H <sub>2</sub> O) <sub>2</sub> H <sup>+</sup> + H <sub>2</sub> O	44.8	10.7	74.5	17.8
12. (MeCOCH <sub>2</sub> CH <sub>2</sub> COMe)(H <sub>2</sub> O) <sub>3</sub> H <sup>+</sup> + H <sub>2</sub> O	40.6	9.7	76.6	18.3
13. (MeCOCH <sub>2</sub> CH <sub>2</sub> COMe)(H <sub>2</sub> O)H <sup>+</sup> + 2H <sub>2</sub> O	97.9	23.4	192.5	46.0
14. (MeCOCH <sub>2</sub> CH <sub>2</sub> COMe) <sub>2</sub> H <sup>+</sup> + H <sub>2</sub> O	63.2	15.1	184.5	44.1
15. (1,4-cyclohexanedione)H <sup>+</sup> + H <sub>2</sub> O	84.5	20.2	112.2	26.8
16. (1,4-cyclohexanedione)(H <sub>2</sub> O)H <sup>+</sup> + H <sub>2</sub> O	56.9	13.6	104.6	25.0
17. (1,4-cyclohexanedione)(H <sub>2</sub> O)H <sup>+</sup> + H <sub>2</sub> O	56.1 <sup>c</sup>	13.4 <sup>c</sup>	(105)	(25)

<sup>a</sup> Uncertainty estimates are derived as in Table 1, with results as follows (reaction number, uncertainty of ΔH° (kJ/mol) and ΔS° (J/(mol K))): 1, 5.9, 13.0; 2, 0.8, 2.1; 3, 2.5, 9.6; 4, 1.7, 7.1; 5, 1.7, 7.1; 6, 1.3, 5.0; 8, 4.2, 10.9, two measurements; 9, 1.7, 5.9, three measurements; 10, 1.7, 6.3, four measurements; 11, 3.4, 11.3, three measurements; 12, 4.6, 15.9; 13, 5.4, 17.6; 14, 6.7, 24.3; 15, 5.0, 11.3; 16, 2.9, 9.2. <sup>b</sup> From ΔG°<sub>221</sub> = -15.5 kJ/mol (-3.7 kcal/mol), ΔS° estimated. <sup>c</sup> From ΔG°<sub>323</sub> = -22.6 kJ/mol (-5.4 kcal/mol), ΔS° estimated.

Substitution of H<sub>2</sub>O by Me<sub>2</sub>CO is unfavorable only when it leads to blocked clusters with weak CH<sub>3</sub><sup>δ+</sup>...O hydrogen bonds, such as in reactions 2 and 3, where ΔH<sub>2</sub><sup>o</sup> = +1.4 kJ/mol (+0.3 kcal/mol) and ΔH<sub>3</sub><sup>o</sup> = +38.2 kJ/mol (+9.1 kcal/mol).



Studies of acetone/water clusters by Iraqi and Lifschitz,<sup>26</sup> Wei et al.,<sup>27</sup> and Szulejko et al.<sup>28</sup> showed that, despite the proposed structure I with water in the center, the cluster loses preferentially H<sub>2</sub>O, rather than Me<sub>2</sub>CO.<sup>26</sup> According to Table 1, H<sub>2</sub>O loss is favored in terms of ΔG°, although it is slightly more endothermic than Me<sub>2</sub>CO loss. This results from a more positive entropy change, which may be due to the loose bonding of the third acetone molecule in the T-shaped product (Me<sub>2</sub>-CO)<sub>3</sub>H<sup>+</sup> ion.

Polar organic molecules usually have higher proton affinities (PAs) than H<sub>2</sub>O. Correspondingly, they can also form stronger ionic hydrogen bonds, as the bond strength of bases B<sub>2</sub> to a constant ion B<sub>1</sub>H<sup>+</sup> increases linearly with PA(B<sub>2</sub>).<sup>3</sup> We examine if this correlation persists in larger systems, by the dissociation energies of the equimolar (B)<sub>3</sub>(H<sub>2</sub>O)<sub>3</sub>H<sup>+</sup> clusters of various bases

(26) Iraqi, M.; Lifschitz, C. *Int. J. Mass Spectrom. Ion Processes* **1986**, *71*, 245.

(27) Wei, S.; Tseng, W. B.; Keese, R. G.; Castleman, J. *Am. Chem. Soc.* **1989**, *111*, 1960.

(28) Szulejko, J. E.; Hop, C. E. C. A.; McMahon, T. B.; Harrison, A. G.; Young, A. B.; Stone, J. A. *J. Am. Soc. Mass Spectrom.* **1992**, *3*, 33.

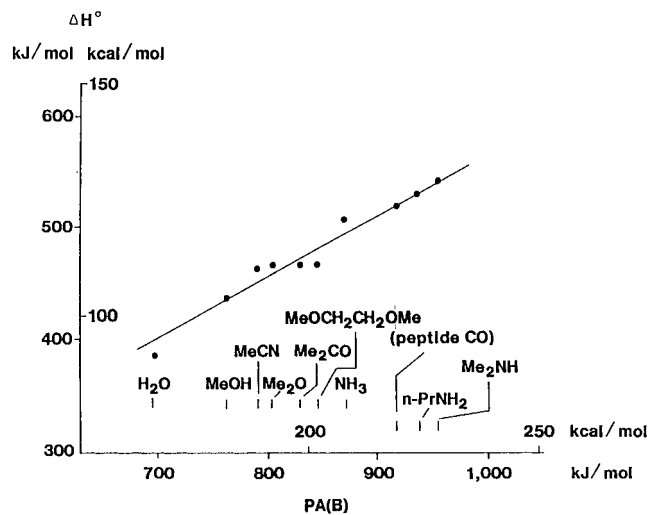
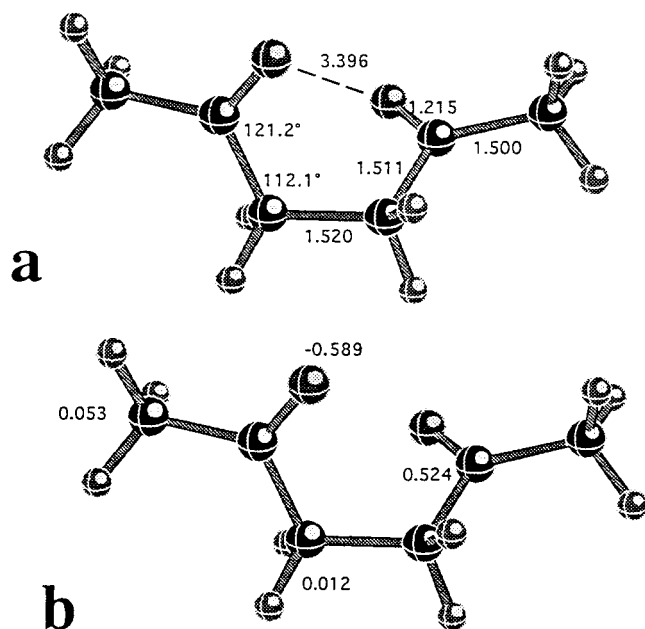
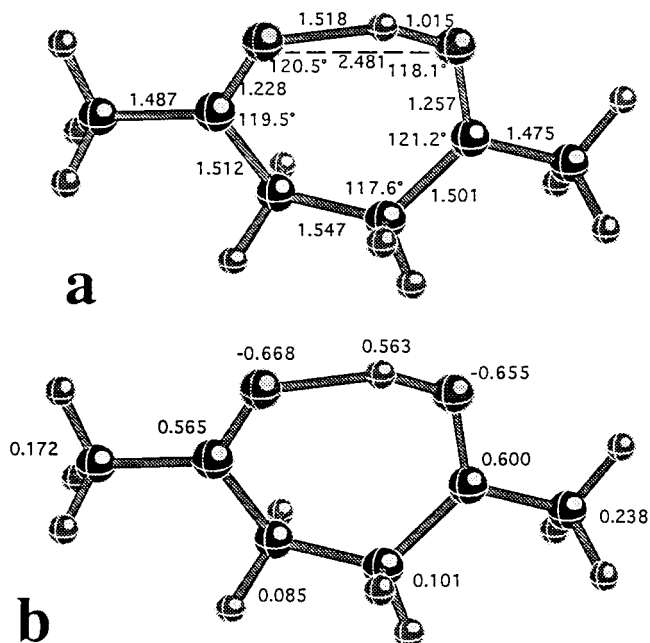


Figure 5. Correlation between the proton affinity of B and the strength of the IHB network as measured by the dissociation energy B<sub>3</sub>(H<sub>2</sub>O)<sub>3</sub>H<sup>+</sup> → H<sub>3</sub>O<sup>+</sup> + 2H<sub>2</sub>O + 3B. For MeOCH<sub>2</sub>CH<sub>2</sub>OMe we use the PA of Et<sub>2</sub>O, 845 kJ/mol (202 kcal/mol), and for MeCONHCH(Me)COOMe, we use the PA of MeCON(Me)<sub>2</sub>, 928 kJ/mol (222 kcal/mol) to represent the functional groups without internal hydrogen bonding. Sources of data for bases b as follows: H<sub>2</sub>O, ref 34; MeOH, ref 29; MeCN, ref 25; Me<sub>2</sub>O, ref 20; Me<sub>2</sub>CO, this work; MeOCH<sub>2</sub>CH<sub>2</sub>OMe, ref 5; NH<sub>3</sub>, ref 1; peptide CO, ref 30; n-PrNH<sub>2</sub> and Me<sub>2</sub>NH, ref 29. Proton affinities are from refs 18 and 31.

B in Figure 5. A linear relation with a slope of 0.56 is observed over a range of >250 kJ/mol (60 kcal/mol) of PA(B). The stabilization of the proton by the overall assembly is linearly



**Figure 6.** (a) Geometry and (b) atomic charges for  $\text{MeCOCH}_2\text{CH}_2\text{-COMe}$ . Charges for  $\text{CH}_2$  and  $\text{CH}_3$  groups are group charges.



**Figure 7.** (a) Geometry and (b) atomic or group charges for  $(\text{MeCOCH}_2\text{CH}_2\text{-COMe})\text{H}^+$ .

related to the PAs of the individual base molecules, even in systems containing several base and water molecules.

**2. Thermochemistry of Diketone/Water Clusters.** The thermochemistry of diketone/water clusters is reported in Table 2. We note first that protonated diketones can form internal hydrogen bonds as illustrated in Figure 7.<sup>32,33</sup> The thermochemistry of the internal bond can be estimated by comparing the protonation energy with those of monofunctional ketones.<sup>31</sup> Clustering displaces and dissociates the internal bonds, requiring positive energy that lowers the overall exothermicity of the clustering reaction. Comparing the dimerization and monohydration energies of  $(\text{MeCOCH}_2\text{COMe})\text{H}^+$  to those of  $\text{Me}_2\text{COH}^+$  gives the internal hydrogen bond strength as 17 kJ/mol (4 kcal/mol) or 19 kJ/mol (5 kcal/mol), respectively. Similarly, for  $(\text{MeCOCH}_2\text{CH}_2\text{-COMe})\text{H}^+$ , we obtain 31 kJ/mol (7 kcal/mol) from both the dimerization and hydration reaction comparisons.

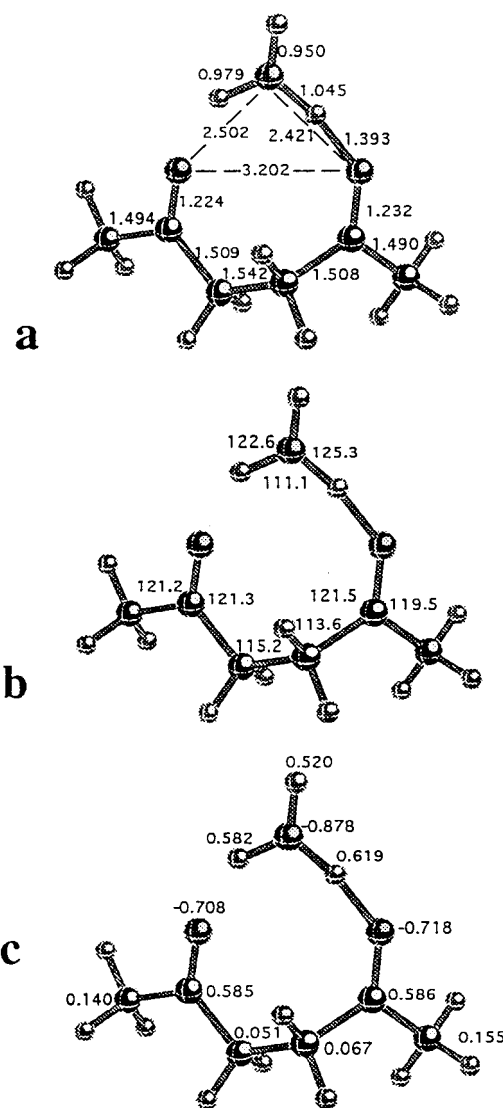


**Figure 8.** (a) Bond lengths, (b) bond angles, and (c) atomic or group charges for  $(\text{MeCOCH}_2\text{CH}_2\text{-COMe})(\text{H}_2\text{O})\text{H}^+$ .

This agrees closely with a previous estimate of 25 kJ/mol (6 kcal/mol) from proton affinity considerations.<sup>32</sup>

In the diether system, as well as in mixed clusters of  $\text{H}_2\text{O}$  with two or more  $\text{MeCN}$ ,  $\text{Me}_2\text{O}$ ,  $\text{Me}_2\text{CO}$ , and  $\text{Me}_3\text{N}$  molecules, the proton remains on a central  $\text{H}_3\text{O}^+$  core ion, although the proton affinities of the bases are higher.<sup>25,27</sup> The present thermochemistry and ab initio results below indicate that this occurs also in the complexes of  $\text{H}_3\text{O}^+$  and  $\text{H}_5\text{O}_2^+$  with the two polar functional groups of the diketones and diamides.

The  $\text{H}_5\text{O}_2^+$  group forms a  $\cdots\text{H}_2\text{O}-\text{H}^+\cdots\text{OH}_2\cdots$  bridge in  $(\text{MeCOCH}_2\text{CH}_2\text{-COMe})(\text{H}_2\text{O})_2\text{H}^+$  as observed in Table 2 by comparing the hydration sequences of the three diketones. Contrary to most clustering sequences, the binding strength for adding the second  $\text{H}_2\text{O}$  molecule does not decrease as usual, but increases slightly. The  $\Delta S^\circ$  value of the second step is also anomalously large. These effects and the subsequent drop in  $\Delta H^\circ$  and  $\Delta S^\circ$  at the third step are consistent with the formation of the bridged structure as shown in Figure 11. The multiple

(29) Meot-Ner (Mautner), M. *J. Am. Chem. Soc.* **1992**, *114*, 3312.

(30) Meot-Ner (Mautner), M. *J. Am. Chem. Soc.* **1984**, *106*, 278.

(31) Lias, S. G.; Liebman, J. F.; Levin, R. D. *J. Phys. Chem. Ref. Data* **1984**, *13*, 695.

(32) Meot-Ner (Mautner), M. *J. Am. Chem. Soc.* **1983**, *105*, 4906.

(33) Yamabe, S.; Hirao, K.; Wasada, H. *J. Phys. Chem.* **1992**, *96*, 10261.

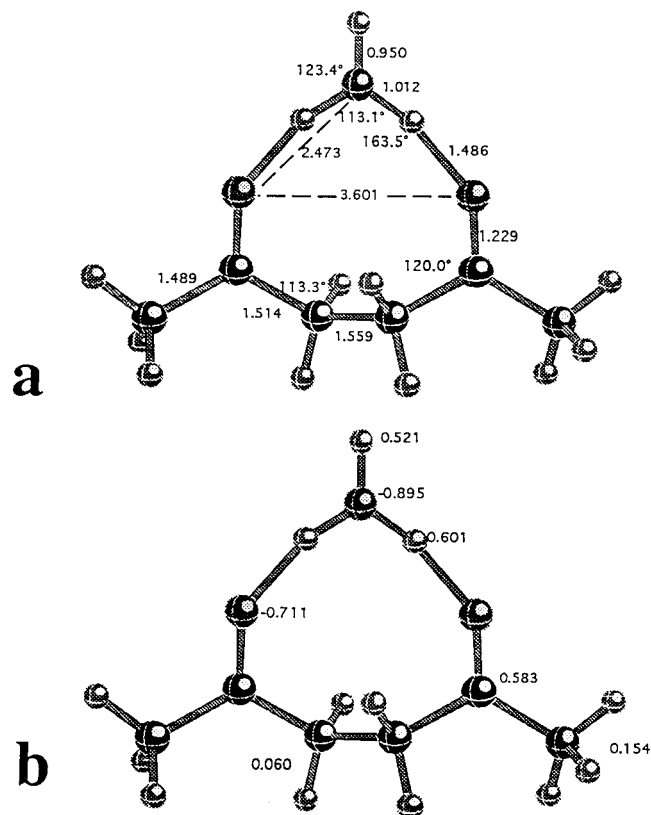


**Figure 9.** (a) Geometry and (b) atomic or group charges for the symmetric transition state for proton transfer in  $(\text{MeCOCH}_2\text{CH}_2\text{COMe})\text{-(H}_2\text{O)}\text{H}^+$ .

hydrogen bonding in this structure enhances the binding energy. The first two  $\text{H}_2\text{O}$  molecules fill a closed solvation shell, after which the subsequent binding energies drop significantly.<sup>28</sup> Similar thermochemistry in the analogous diether system  $(\text{MeOCH}_2\text{CH}_2\text{OMe})(\text{H}_2\text{O})_2\text{H}^+$  was also shown by ab initio calculations to be associated with a bridged structure.<sup>5</sup> A similar effect is observed in the hydration of (1,4-cyclohexanedione)- $\text{H}^+$ , where the two carbonyls are sufficiently removed to allow a  $\text{CO}\cdots\text{H}_2\text{OH}^+\cdots\text{OH}_2\cdots\text{OC}$  bridge between them. However, the data are limited because of volatility problems.

For comparison, in the more constrained  $(\text{MeCOCH}_2\text{COMe})\text{-(H}_2\text{O})_2\text{H}^+$ , the geometry is unfavorable for a bridge of two  $\text{H}_2\text{O}$  molecules. Table 2 shows a monotonic decrease in hydration energies toward the usual limit of  $40 \pm 4$  kJ/mol ( $9.5 \pm 1$  kcal/mol) in this hydration series, and  $\Delta S^\circ$  values also show no anomaly that would suggest a bridged structure.

**3. Ab Initio Calculations of Solvent-Bridged Diketone and Diamide Systems.** The ab initio calculated energies are reported in Table 3. The calculated ab initio geometries and charge distributions of the neutral, protonated, and monohydrated and dihydrated protonated diketones are illustrated in Figures 6–12, and of a model protonated diamide, in Figure 13.

The thermochemical anomaly noted in  $(\text{MeCOCH}_2\text{CH}_2\text{COMe})(\text{H}_2\text{O})_2\text{H}^+$  is within the experimental error and cannot prove unequivocally a bridged structure. However, structural information on complex and internally hydrogen-bonded ions can be obtained also computationally, as was done by Yamabe et al. on difunctional ions.<sup>33</sup> We performed ab initio calculations on the present diketone, in its neutral, protonated, and monohydrated and dihydrated forms. The 4-31G basis set was used for several reasons. First, its computational efficiency allowed a thorough search of the conformational space of each complex,

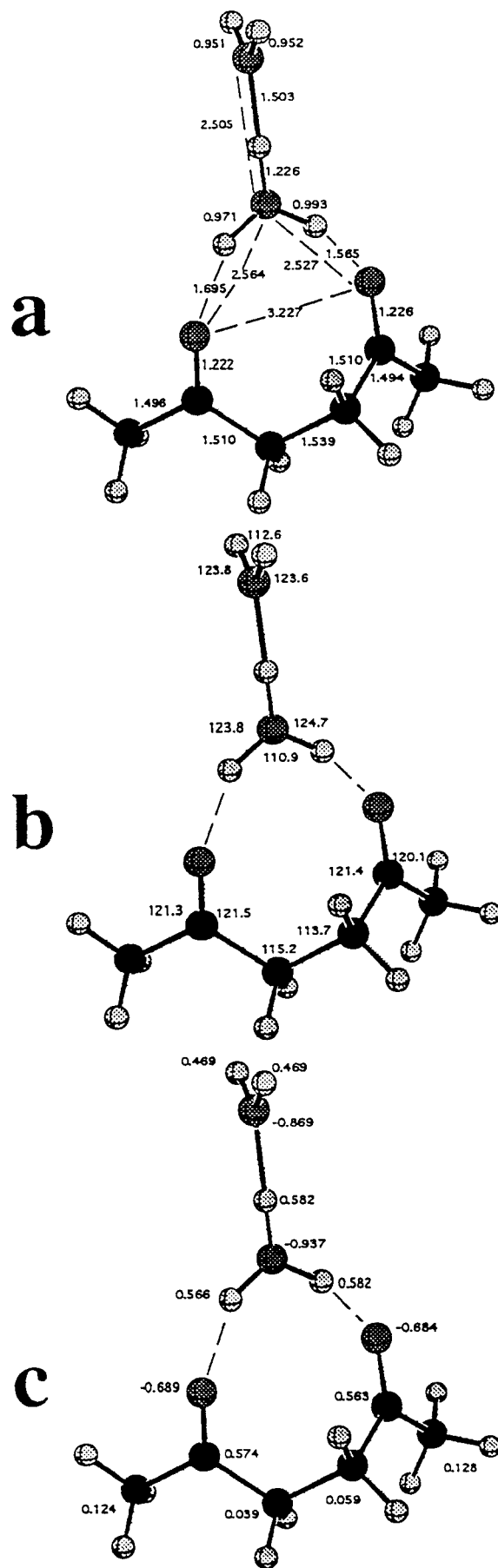


**Figure 10.** (a) Bond lengths, (b) bond angles, and (c) atomic or group charges for the one-water bridged complex  $(\text{MeCOCH}_2\text{CH}_2\text{COMe})\text{-(H}_2\text{O})_2\text{H}^+$ .

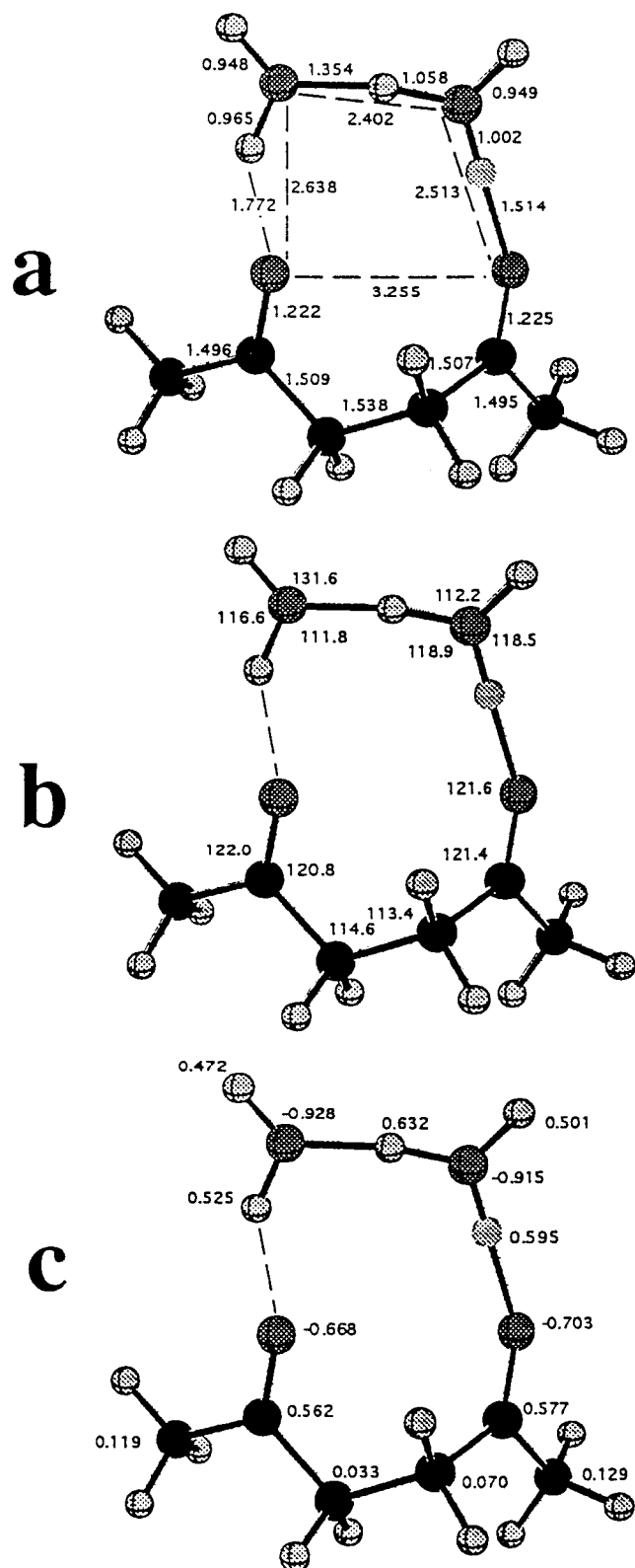


**Figure 11.** (a) Bond lengths, (b) bond angles, and (c) atomic or group charges for the two-water bridged complex (MeCOCH<sub>2</sub>CH<sub>2</sub>COMe)-(H<sub>2</sub>O)<sub>2</sub>H<sup>+</sup>.

particularly important for surfaces which are very flat in some dimensions. The computed complexation energies can be surprisingly accurate, especially for complexes dominated by electrostatic interactions.<sup>24,35–37</sup> Another advantage of the

(34) Meot-Ner (Mautner), M.; Speller, C. V. *J. Phys. Chem.* **1986**, *90*, 6616.

4-31G basis set at the SCF level is that the proton-transfer barriers are typically quite similar to those obtained with much larger sets and with correlation added.<sup>24,38,39</sup> Finally, there exists a prior study which evaluated the barrier to proton transfer between water molecules with this basis set, for a variety of interoxygen distances, with which the results here may be compared directly.<sup>39</sup> We also observe that the calculated protonation and complexation energetics for the present species, summarized in Table 3, agree very well with experimental values.

In the unsolvated diketone, the addition of a proton forms a hydrogen bond between the two O atoms and shortens the O–O distance from 3.396 Å in the neutral molecule to 2.481 Å in the protonated species (Figures 6 and 7). This geometry is somewhat less tight than the lower-level RHF/3-21G geometries calculated by Yamabe et al.<sup>33</sup> The hydrogen bond is strongly asymmetric, which suggests a significant barrier to proton transfer.

It is interesting to compare the effects of actual full protonation and of partial protonation by hydrogen bonding to a proton of the H<sub>3</sub>O<sup>+</sup> ion. First, the proton binds by 885 kJ/mol (211.5 kcal/mol) to the diketone and transfers to it 0.437 of a unit charge, while H<sub>3</sub>O<sup>+</sup> binds by 249 kJ/mol (59.5 kcal/mol) and transfers only 0.157 of a unit charge to the diketone.

Binding of the proton is highly asymmetric with two bonds, of 1.02 and 1.52 Å, as in Figure 7. In comparison, two protons of H<sub>3</sub>O<sup>+</sup> bond to the diketone and form a more symmetrical geometry, with two hydrogen bonds of 1.39 and 1.54 Å. In fact, the asymmetry could disappear at higher level MP calculations.<sup>40</sup> The proton brings the two ketone oxygens closer by 0.915 Å compared with the neutral, while the H<sub>3</sub>O<sup>+</sup> ion brings them closer only by 0.194 Å. Protonation stretches the C=O bond by 0.042 Å, while the H<sub>3</sub>O<sup>+</sup> ion interaction, only by 0.017 Å. Other notable effects are a stretching of the CH<sub>2</sub>–CH<sub>2</sub> bond by 0.027 Å and increase of the (H<sub>2</sub>)C–C(H<sub>2</sub>)–C(O) bond angle by 5.1° by protonation, compared with somewhat smaller changes of 0.022 and 1.5 Å in the H<sub>3</sub>O<sup>+</sup> adduct. Also of interest is that the methyl groups are important in charge delocalization from the ion, in that the total positive charge on the two methyl groups increases by 0.304 unit charge upon protonation and by 0.193 in the H<sub>3</sub>O<sup>+</sup> adduct.

In general, the geometries of the H<sub>5</sub>O<sub>2</sub><sup>+</sup> adducts are similar to the H<sub>3</sub>O<sup>+</sup> adducts. An exception is that in the bridged structure in Figure 11: the two CO oxygens interact with two widely spaced H atoms, and the ketone oxygen distance stretches by 0.053 Å compared with that of the H<sub>3</sub>O<sup>+</sup> adduct.

The most important feature is that the proton remains on the H<sub>3</sub>O<sup>+</sup> center. Displacement of the H<sub>3</sub>O<sup>+</sup> cation to a symmetric position gives a saddle point with equivalent water–ketone R(O···O) distances of 2.47 Å and a concomitant stretch of 0.4 Å in the distance between the ketone oxygens. This transition state creates an energy barrier of 9.2 kJ/mol (2.2 kcal/mol) for proton transfer in the monohydrated complex. The low barrier may result in part from partial compensation between the unoptimized geometry that raises the energy of the transition state and the somewhat increased charge delocalization from H<sub>3</sub>O<sup>+</sup> to the diketone, of 0.172 unit charge compared with 0.157

(35) Rohlfing, C. M.; Allen, L. C.; Cook, C. M.; Schlegel, H. B. *J. Chem. Phys.* **1983**, *78*, 2498.

(36) Desmeules, P. J.; Allen, L. C. *J. Chem. Phys.* **1980**, *72*, 4731.

(37) Scheiner, S.; Harding, L. B. *J. Am. Chem. Soc.* **1981**, *103*, 2169.

(38) Scheiner, S.; Szczesniak, M. M.; Bigham, L. D. *Int. J. Quantum Chem.* **1983**, *23*, 739.

(39) Scheiner, S. *J. Am. Chem. Soc.* **1981**, *103*, 315.

(40) Scheiner, S.; Szczesniak, M. M. *J. Chem. Phys.* **1982**, *77*, 4586.

**Table 3.** Calculated ab Initio 4-31G vs Experimental Thermochemistry of Protonation and Complexation of MeCOCH<sub>2</sub>CH<sub>2</sub>COMe<sup>a</sup>

	$-\Delta E_{\text{elec}}$	$-\Delta H^{\circ}_{298}$	$-\Delta H^{\circ}_{\text{exp}}$	$-\Delta S^{\circ}_{298}$	$-\Delta S^{\circ}_{\text{exp}}$
MeCOCH <sub>2</sub> CH <sub>2</sub> COMe + H <sup>+</sup>	915.9	884.9	888.7	124.7	136.0
MeCOCH <sub>2</sub> CH <sub>2</sub> COMe + H <sub>3</sub> O <sup>+</sup>	251.5	249.0	246.5	145.6	151.5
MeCOCH <sub>2</sub> CH <sub>2</sub> COMe + H <sub>5</sub> O <sub>2</sub> <sup>+</sup> <sup>b</sup>	179.5	164.8	168.2	141.4	176.6
MeCOCH <sub>2</sub> CH <sub>2</sub> COMe + H <sub>3</sub> O <sub>2</sub> <sup>+</sup> <sup>c</sup>	173.2	162.3	168.2	152.3	176.6
MeCONHCH <sub>2</sub> CONH <sub>2</sub> + H <sub>5</sub> O <sub>2</sub> <sup>+</sup>	202.1	191.2	(185) <sup>d</sup>	168.2	

<sup>a</sup>  $E_{\text{elec}}$  and  $\Delta H^{\circ}$  in kJ/mol,  $\Delta S^{\circ}$  in J/(mol K). Experimental data from refs 25–27 and present work and thermochemical cycles. <sup>b</sup> Single H<sub>2</sub>O bridge as shown in Figure 10. <sup>c</sup> Double H<sub>2</sub>O bridge as shown in Figure 11. <sup>d</sup> Experimental  $\Delta H^{\circ}$  estimated from a thermochemical cycle using the proton affinity of MeCONHCH<sub>2</sub>COOMe and the hydration energy of (MeCONHCH(CH<sub>3</sub>)COOMe)H<sup>+</sup> by two H<sub>2</sub>O molecules from ref 30.

unit charge transferred in the ground-state geometry, which decreases the energy of the transition state.

Adding a further H<sub>2</sub>O molecule can result in two structures of nearly equal energy. One, in Figure 10, adds to the third, unbound proton of H<sub>3</sub>O<sup>+</sup> and slightly attracts the hydrogen-bonding protons away from the ketone oxygens, stretching the hydrogen bonds by 0.106 and 0.062 Å. The ketone R(O···O) distance also stretches, closer to the neutral value than in the complex with H<sub>3</sub>O<sup>+</sup> alone. These changes suggest weaker hydrogen bonds from H<sub>3</sub>O<sup>+</sup> to the ketone, and in fact, the binding energy of H<sub>5</sub>O<sub>2</sub><sup>+</sup> to the diketone is weaker by 84 kJ/mol (20 kcal/mol) than of H<sub>3</sub>O<sup>+</sup> alone. The stronger bonding energy of H<sub>3</sub>O<sup>+</sup> vs H<sub>5</sub>O<sub>2</sub><sup>+</sup> results from the more concentrated charge on the smaller cation.

More interesting as a water-bridged model is the complex in Figure 11. Compared with Figure 10, it gives a less symmetric structure, where the shorter OH···O distance has contracted from 2.527 to 2.513 Å, while the longer bond ketone–water OH···O distance has stretched from 2.564 to 2.638 Å, suggesting somewhat weaker ketone–water bonding in the two-water bridged structure. On the other hand, the inter-water OH···O distance is shorter, only 2.402 vs 2.505 Å, suggesting a stronger bond. The longer bridge allows the two ketone O atoms to move apart from 3.227 Å to a less strained 3.255 Å. The net result is that the energies of the two (MeCOCH<sub>2</sub>CH<sub>2</sub>COMe)-(H<sub>2</sub>O)<sub>2</sub>H<sup>+</sup> structures are comparable, with the second being less stable by 6.3 kJ/mol (1.5 kcal/mol) in  $\Delta E_{\text{elec}}$  and 2.5 kJ/mol (0.6 kcal/mol) in  $\Delta H^{\circ}$ . The two-water bridged structure in Figure 11 is more constrained and has a more negative calculated  $\Delta S^{\circ}$  value, closer to the experimental result. Calculations show that clusters may often involve equilibrium mixtures of isomers of close energy,<sup>34,41</sup> and the two structures in Figures 10 and 11 may be also present in equilibrium mixtures.

The calculated 4-31G energy barrier to proton transfer in the two-water bridged structure, through the transition state shown in Figure 12, is 12.1 kJ/mol (2.9 kcal/mol). At the same level of the theory, there is no barrier for proton transfer in H<sub>5</sub>O<sub>2</sub><sup>+</sup>, which contains a centrosymmetric hydrogen bond.<sup>39</sup> The barrier in the complex with the diketone may be due to presence of the extra, unsymmetric hydrogen bonds to the ketone oxygens, which weaken and lengthen the central bond. With respect to the calculated barrier heights, it is commonly observed that barriers to proton transfer rise as the basis set is enlarged and diminish when correlation is included.<sup>40</sup> As a result, it is not uncommon for 4-31G barriers to correspond fortuitously closely with values computed with much more sophisticated approaches.

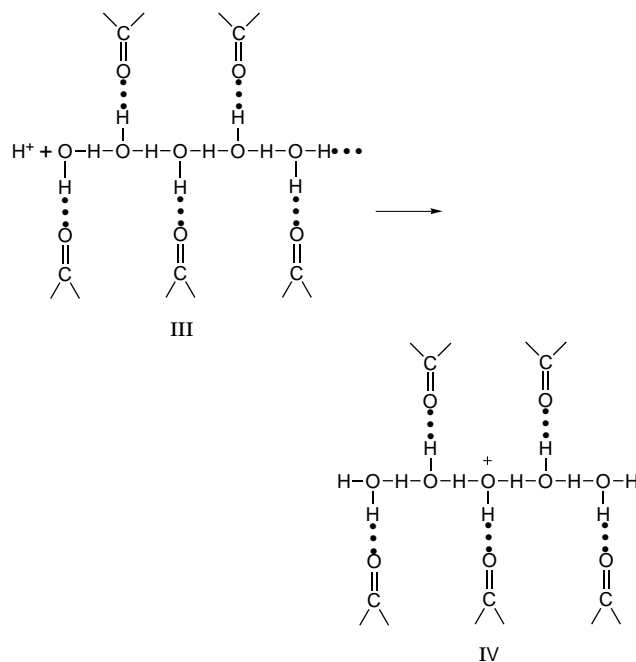
The important point is the small magnitude of the barrier. In comparison, without the water molecules, the intramolecular bond in Figure 7, whose strength was estimated as 29 kJ/mol (7 kcal/mol), would have to be disrupted for proton movement posing a large barrier.

An even smaller barrier is found in the water bridge in a diamide system, as shown in Figure 13. This system is

unsymmetrical, but transfer of the proton to the left-hand H<sub>2</sub>O molecule yields a second minimum higher only by 2.0 kJ/mol (0.47 kcal/mol) than the conformation shown. This second minimum is extremely shallow and is separated from the first by a barrier less than 0.4 kJ/mol (0.1 kcal/mol), too small to contain a vibrational level. Therefore the complex can be considered to contain a single minimum, allowing proton transfer from one H<sub>2</sub>O molecule to the other virtually without an energy barrier.

**4. Cluster Analogues of Energy Components in Membrane Transport.** The mixed clusters above are similar to protonated water wires in proteins as both contain hydrogen bond networks of carbonyl groups and water molecules. However, there are also obvious differences. In particular, the surrounding polar solvent and protein can make major energy contributions in proteins, as shown, for example, in Warshel's models of rhodopsin proton pumps and in models of ion transport.<sup>8–11</sup> There are also differences in size of the biological assembly vs the clusters, in the contributions of amide vs ketone groups, and in geometry, although some of these differences may approximately cancel (see the Appendix). While the clusters cannot yield quantitative bioenergetics, they provide mechanistic insights and a measure of the contributing energy physical factors.

**a. Stability of the Hydrogen Bond Network and Contributions of Amide Carbonyls.** The entry of protons to the water wire is depicted schematically by structures III and IV.



When one hydrogen atom in each H<sub>2</sub>O molecule is bonded to another H<sub>2</sub>O molecule and the other to a protein carbonyl, the assembly is an equimolar water/carbonyl mixture. The



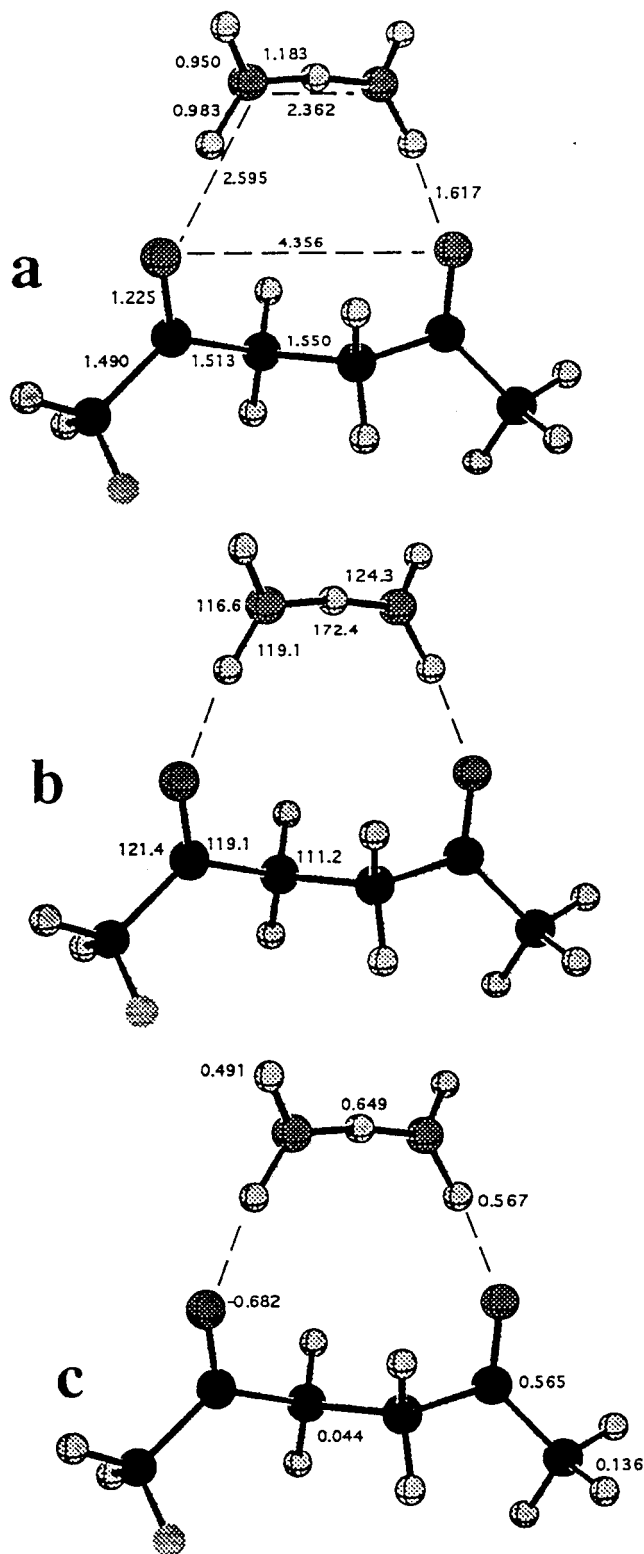


**Figure 12.** (a) Bond lengths, (b) bond angles, and (c) atomic or group charges for the symmetric transition state for proton transfer in  $(\text{MeCOCH}_2\text{CH}_2\text{COMe})(\text{H}_2\text{O})_2\text{H}^+$ .

largest measured equimolar cluster in this work,  $(\text{Me}_2\text{CO})_3(\text{H}_2\text{O})_3\text{H}^+$ , serves as a model. Fortunately, the five hydrogen bonds in the cluster contain most of the specifically ionic interactions.<sup>2,3</sup> The analogy to biological models and clusters is illustrated by a detailed electrostatic model of  $\text{Na}^+$  in the gramicidin channel that also involves six immediate polar neighbors.<sup>11</sup>

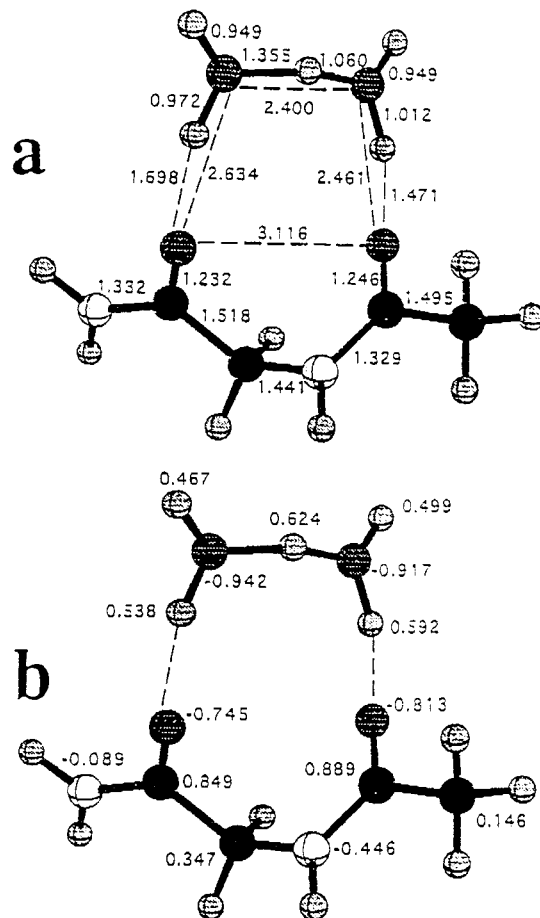
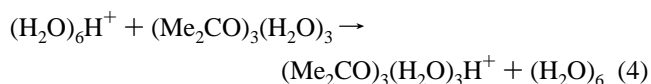


**Figure 13.** (a) Bond lengths and (b) atomic or group charges for the two-water bridged diamide complex  $(\text{MeCONHCH}_2\text{CONH}_2)(\text{H}_2\text{O})_2\text{H}^+$ .

The cluster model for proton transfer from neat water into the wire is represented by reaction 4.



The enthalpy change of reaction 4 is equal to  $\Delta H^\circ_4$ , assuming that the five  $\text{OH}\cdots\text{O}$  hydrogen bonds on each side of eq 5 are approximately equal:



This exothermicity can be obtained from Table 1 as  $-80$  kJ/mol ( $-19$  kcal/mol), and it reflects the extra stabilization of the proton by the carbonyl groups. As a model, it can represent ion-dipole hydrogen bonds as a theoretical isolated energy factor in the membrane channel, as they would be in the absence of other energy components (different factorings of energy components are of course also possible).<sup>11</sup>

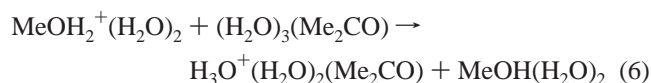
To model the condensed-phase biological system more closely, the corrections in the Appendix and the effects of the water and protein dielectric medium should be evaluated.<sup>8-11</sup> Additional interactions of the hydrogen-bonding groups can weaken the ionic hydrogen bonds between the  $\text{H}_2\text{O}$  molecules and protein carbonyl groups,<sup>42,43</sup> and the cluster values indicate the upper limits. Qualitatively, the observed strong hydrogen bonds support the importance of peptide carbonyl interactions in proton transport.<sup>8-11</sup>

**b. Contributions Assisting a Delocalized Proton.** In proton transport, it is essential that the proton can remain delocalized,

i.e. that it should not be trapped by strongly basic amide groups. We observe that in the model clusters the proton is located on an  $\text{H}_3\text{O}^+$  center and the charge is retained largely by this center. In the complex with  $\text{MeCOCH}_2\text{CH}_2\text{COMe}$  in Figure 8, the  $\text{H}_3\text{O}^+$  ion retains 0.843 of a unit charge and the  $\text{H}_5\text{O}_2^+$  groups retain 0.862 and 0.882 unit charges in Figures 10 and 11, respectively, even in the presence of the polar and strongly polarizable ligand. This results from the electrostatic balance of the proton in a central location between opposing carbonyl dipoles. Similar balancing attractions of surrounding protein dipoles can allow the proton to remain delocalized and mobile in the central water wire and avoid trapping by the basic polar groups.

**c. Energetics of Proton Transport.** In the two-water bridged cluster  $(\text{MeCOCH}_2\text{CH}_2\text{COMe})(\text{H}_2\text{O})_2\text{H}^+$  in Figure 11 and in the bridged diamide/water cluster in Figure 13, the calculations indicate only a small or negligible barrier to proton transfer between the water molecules. A similar effect may facilitate proton transport along the water chain in membranes. The low barrier requires that the effective  $\text{p}K_a$ 's of the water molecules along the chain are close. This is achieved again by the balancing effects of opposing surrounding polar groups.

In some proton wires, serine or tyrosine hydroxyl groups may participate.<sup>44,45</sup> A problem in mixed  $\text{H}_2\text{O}$  and ROH chains may be proton transfer from the  $\text{ROH}_2^+$  ion, since the proton affinities of alcohols are higher than those of  $\text{H}_2\text{O}$  by 54–92 kJ/mol (13–22 kcal/mol).<sup>31</sup> However, the difference can be balanced by the additional bond that  $\text{H}_3\text{O}^+$  can form with peptide CO groups. This effect is illustrated by the endothermicity of proton transfer from  $\text{MeOH}_2^+$  to  $\text{H}_2\text{O}$ , 64 kJ/mol (15 kcal/mol), which is reduced to 3.4 kJ/mol (0.8 kcal/mol) in the analogous cluster reaction 6 (assuming all neutral  $\text{OH}\cdots\text{O}$  bond strengths of 21 kJ/mol (5 kcal/mol)).<sup>1,29</sup>



This example illustrates that hydrogen bonding to the carbonyl groups effectively brings the proton affinity of the  $\text{H}_2\text{O}$  molecule close to that of the alcohol. A similar effect can allow the proton to move from alcohol to water molecules in mixed  $\text{H}_2\text{O}$  and ROH chains.

## Conclusions

Thermochemical and computational observations on protonated ketone/water clusters are analogous to components of the water wire system that conduct protons through protein channels in membranes.

Together with previous results on anions,<sup>6,7</sup> the present data show that ionic intermediates can be strongly stabilized by hydrogen bonds to surrounding peptide NH and CO groups. These bonds, as a theoretical isolated energy component, can stabilize the ionic charge by up to 135 kJ/mol (32 kcal/mol). The strong interactions are possible because peptide amide links are strong intrinsic CO bases and NH acids, which makes them strong hydrogen bond acceptors and donors, respectively.

The strong ionic hydrogen bonds in the clusters suggest possible analogous roles in proton transport.

(42) Meot-Ner (Mautner), M.; Hamlet, P.; Hunter, E. P.; Field, F. H. *J. Am. Chem. Soc.* **1980**, *102*, 6866.

(43) Meot-Ner (Mautner), M. *J. Phys. Chem.* **1987**, *91*, 417.

(44) Onsager, L. *Science*, **1967**, *156*, 541.

(45) Zundel, G. In *Transport through Membranes: Carriers, Channels and Pumps*; Pullman, A., Ed.; Kluwer: Dordrecht, The Netherlands, 1988; p 409.

1. The ketone/water clusters show the special stability of  $\text{H}_3\text{O}^+(\text{Me}_2\text{CO})_2$  units, even in larger clusters. The stabilization of the hydrogen bond network increases with acetone content. As a result, proton transfer from neat water clusters to the ketone/water clusters is significantly exothermic. In analogy, proton transfer from the aqueous environment to the polar protein environment of the water wire can be facilitated by ionic hydrogen bonds to the carbonyl groups that stabilize the proton by 80 kJ/mol (19 kcal/mol) in the model reaction 4 above. This effect can be amplified or compressed by further hydrogen bonding and by dielectric solvent effects of the protonated center. The strong observed stabilizing effects of the carbonyl interactions support the role ascribed by Warshel to protein permanent dipoles.<sup>8–11</sup>

2. In the mixed clusters, the proton and much of its charge density remain on an  $\text{H}_3\text{O}^+$  center. This is indicated by the stability of the  $\text{H}_3\text{O}^+(\text{Me}_2\text{CO})_2$  group, by collisional dissociation studies on mixed clusters,<sup>26–28</sup> and by computations. The central position of the proton is due to the balancing electrostatic forces of opposing carbonyl dipole moments. Similar factors may allow the proton to remain on an  $\text{H}_3\text{O}^+$  center in water wires. This effect allows the proton to avoid trapping by the strongly basic protein amide groups and to remain delocalized and mobile in the water chain through the membrane.

3. Protonated water bridges are indicated in the  $(\text{MeCOCH}_2\text{CH}_2\text{COMe})(\text{H}_2\text{O})_2\text{H}^+$  cluster and in the analogous diether and diamide clusters, with low barrier to proton transfer. Similar protonated water bridges and chains can provide pathways for proton transport with low energy barriers in membranes. Calculations are necessary to examine if water bridges preserve this feature in larger systems.

Cluster models illustrate several significant roles of ionic hydrogen bonds in membranes, in enzyme active centers,<sup>6,7</sup> and in neurotransmitter–receptor interactions.<sup>48</sup> The cluster data can provide mechanistic insights and can also help calibrate quantitatively theoretical computations to test the proposed energy contributions of ionic hydrogen bonds in biological systems.

**Acknowledgment.** The work by the SIU authors was supported by Grant GM29391 from the National Institutes of Health.

## Appendix: Correction Estimates for the Cluster Model

Cluster measurements show that the ionic interactions of a protonated center are contained mostly in specific hydrogen bonds to the four to six neighboring molecules.<sup>2,3</sup> Therefore these specific ionic hydrogen bond contributions, separated theoretically from other effects (see below), may be modeled by clusters if the structural differences between the clusters and the components of the biosystem can be estimated.

**a. Cluster Size.** The model above uses the  $(\text{Me}_2\text{CO})_3\text{-(H}_2\text{O)}_3\text{H}^+$  cluster, which is the largest measurable equimolar cluster. Fortunately, previous studies showed that ionic interactions are concentrated primarily in binding to the first four to six ligand molecules.<sup>2,3</sup> Beyond this ionic core, further binding energies approach those in the neutral liquid.<sup>29,43</sup> Therefore, increasing the cluster size should not affect the thermochemistry of reaction 4 significantly. In fact, the data in Table 1 show

(46) Hiraoka, K.; Morise, T.; Nishijama, S.; Nakamura, M.; Nakazato, M.; Ohkuma, K. *Int. J. Mass Spectrom. Ion Phys.* **1986**, *68*, 99.

(47) Hiraoka, K.; Takimoto, H.; Morise, K.; Shoda, T.; Nakamura, S. *Bull. Chem. Soc. Jpn.* **1986**, *59*, 2247.

(48) Deakyne, C. A.; Meot-Ner (Mautner), M. *J. Am. Chem. Soc.* **1998**, submitted.

that, even for the analogous reactions in smaller clusters,  $\Delta H^\circ$  values are similar. For reactions analogous to reaction 4 with two-, four-, and six-membered clusters, values are  $-86.2$ ,  $-82.4$ , and  $-80.0$  kJ/mol ( $-20.6$ ,  $-19.7$ , and  $-19.1$  kcal/mol, respectively).

As an alternative to the  $(\text{Me}_2\text{CO})_3(\text{H}_2\text{O})_3\text{H}^+$  cluster, in analogy with the model of Aquist and Warshel for  $\text{Na}^+$  transport in gramicidin that contains four amide CO groups and two  $\text{H}_2\text{O}$  molecules about an  $\text{Na}^+$  ion,<sup>11</sup> the  $(\text{Me}_2\text{CO})_4(\text{H}_2\text{O})_2\text{H}^+$  cluster could best represent the proton in the gramicidin channel. According to Table 3, this would ascribe an additional 18.0 kJ/mol (4.3 kcal/mol) stabilization by hydrogen bonding.

**b. Composition.** For volatility reasons, the peptide amide carbonyl groups are simulated by ketones. However, the actual protein amide CO groups have higher proton affinities than acetone and should therefore be stronger hydrogen acceptors.<sup>3</sup> The correlation in Figure 5 suggests that the total hydrogen bond strength in the  $(\text{peptide CO})_3(\text{H}_2\text{O})_3\text{H}^+$  network compared with the model  $(\text{Me}_2\text{CO})_3(\text{H}_2\text{O})_3\text{H}^+$  should be increased by 49 kJ/mol (12 kcal/mol). The correction in going from ketone to amide carbonyls can be also estimated from comparing the ab initio binding energy of  $\text{H}_5\text{O}_2^+$  to a diketone vs diamide in Table 3. The correction of 29 kJ/mol (7 kcal/mol) for two carbonyl groups extrapolates to about 42 kJ/mol (10 kcal/mol) for three carbonyl groups, consistent with the estimate based on proton affinities.

**c. Geometry.** The model clusters are free to achieve optimized three-dimensional structures, while the water in protein channels is constrained to the geometry of a chain, shown schematically in ion IV in section 4a above. The possible energy effects are illustrated by ab initio energies of linear and branched  $(\text{MeCN})_2(\text{H}_2\text{O})_2\text{H}^+$  clusters which differ by 8–16 kJ/mol (2–4 kcal/mol) or linear and branched  $(\text{H}_2\text{O})_4\text{H}^+$  or  $(\text{NH}_3)_4\text{H}^+$  isomers whose energies differ by 13–21 kJ/mol (3–5 kcal/mol).<sup>25,41</sup>

Another pertinent observation is obtained from the dissociation energy of the constrained assembly  $(\text{MeCOCH}_2\text{CH}_2\text{COMe})-(\text{H}_2\text{O})_2\text{H}^+$  to  $\text{H}_3\text{O}^+$  and neutrals (from a thermochemical cycle and the data of Table 2 and refs 31 and 32), which is 301 kJ/mol (72 kcal/mol), smaller by 68 kJ/mol (16 kcal/mol) than of the analogous optimized cluster  $(\text{Me}_2\text{CO})_2(\text{H}_2\text{O})_2\text{H}^+$ . On the average, the unoptimized linear geometry seems to weaken the ionic hydrogen bond system by  $42 \pm 20$  kJ/mol ( $10 \pm 5$  kcal/mol). This approximately compensates for the correction due to the increased proton affinities of the amide groups.

Altogether, the size, composition, and geometry corrections in going from the optimized  $(\text{Me}_2\text{CO})_3(\text{H}_2\text{O})_3\text{H}^+$  cluster to a larger  $(\text{peptide CO})_n(\text{H}_2\text{O})_n\text{H}^+$  with a protein geometry may be relatively small and compensating, so that the values derived from the cluster model may be valid for the ionic core in the water wire/protein assembly within  $\pm 20$  kJ/mol ( $\pm 5$  kcal/mol).

The cluster energetics may therefore give a semiquantitative indication of the hydrogen bond contributions in a membrane system. Quantitative application to the actual biosystem will be possible only when the contributions of the bulk dielectric medium can be also calculated.

With respect to assigning energy components, such as the contributions of specific hydrogen bonds, note that these energy components do not exist separately in the interacting system. Such factors as electrostatic and covalent energy contributions to a given bond, or the strength of an individual bond in a system where the strengths of bonds are mutually affected, cannot be measured separately when the only measurable entity is the overall energy of the system. Applied to membrane systems, the contributions assigned to individual hydrogen bonds in a complex cluster or biosystem by any model cannot be tested experimentally, and any reasonable assignment, depending on the definitions, is equally valid. Nevertheless, of course, the assignment of energy components is valuable in theoretical analysis.

JA971663S